

DETERMINATION OPTIMUM Ni CONCENTRATION IN Zn₂SnO₄/Ni-DOPED Sb₂S₃ THIN FILMS WITH DIFFERENT Ni CONCENTRATIONS USING INCIDENT PHOTONS TO CURRENT EFFICIENCY (IPCE) AND CURRENT DENSITY (J) - VOLTAGE (V) MEASUREMENTS

S. NAR^a, O. SAHIN^b, S. HOROZ^{c*}

^a*Siirt University, Institute of Science and Technology, 56100, Siirt, Turkey*

^b*Siirt University, Faculty of Engineering, Department of Chemical Engineering, 56100, Siirt, Turkey*

^c*Siirt University, Faculty of Engineering, Department of Electrical and Electronics Engineering, 56100, Siirt, Turkey*

In this present study, Ni-doped Sb₂S₃ thin films with different Ni concentrations were synthesized on Zn₂SnO₄ coated with FTO conductive glasses by CBD method at room temperature using Ni as the dopant material. The concentration of Ni to be doped during the experiment was determined as 0.25%, 0.5%, 0.75%, and 1%. In the first stage of this study, incident photons to current efficiency (IPCE) and current density (J) - voltage (V) measurements were conducted to investigate the photovoltaic properties of Zn₂SnO₄/Ni-doped Sb₂S₃ thin films with different Ni concentrations for the first time. The main reason for performing IPCE and J-V measurements is to determine Ni-doped Sb₂S₃ thin film with optimum Ni concentration with the best solar cell performance. It was found that Sb₂S₃:Ni(0.75%) thin film has the highest IPCE (%) and power conversion efficiency values compare to other Ni concentrations.

(Received July 9, 2018; Accepted October 11, 2018)

Keywords: Characterization, Doping, Photovoltaic, Synthesis, Thin film

1. Introduction

The constant increase in population causes energy shortage and environmental pollution in the world [1]. Reduction of natural resources such as oil, coal, and gas due to demand-supply imbalance has led people to investigate alternative energy sources [2]. Hydrogen, wind, tidal and sunshine are among the alternative energy sources [3-4]. Compared to other sources, solar energy is considered to be an inexpensive and non-consumable alternative [5]. In the photovoltaic technology where solar energy is used as a source, the sunlight is captured by an absorber material [6]. Organic solar cells [7], dye-sensitized solar cells [8], concentrator solar cells [9] and quantum dot sensitized solar cells [10] are the most advanced configurations of solar cells available today. Cost and efficiency are two key concepts that the solar cell industry focuses on [10]. Thin-film solar cells with the advantages of low cost, easy manufacturing, and low material usage, provide an efficiency of 19% [11].

In thin film technology, there has recently been an increased interest in the V-VI group of semiconductor materials [12-13], which have appropriate optical and electrical properties. Among them, antimony trisulfide (Sb₂S₃) in the stibnite phase has been used in different application areas such as optoelectronics and switching devices [14]. Sb₂S₃ with high absorption coefficient and a refractive index has an energy band gap ranging between 1.5 and 2.2 eV [15] and is used as a good absorber in photovoltaic applications. Sb₂S₃ has been used for solar cell structures such as Ag Sb₂S₃:C/CdS/ITO [16], Pt- Sb₂S₃[17] and n- Sb₂S₃/p-Ge [18] and the average efficiency has been calculated as 7.4%.

One of the ways to improve the optical and electrical properties of semiconductors and their solar cell efficiency is to be doped them with the appropriate material [19]. Transition metals

*Corresponding author: sabithoroz@siirt.edu.tr

such as manganese (Mn) [20], nickel (Ni) [21], cobalt (Co) [22], iron (Fe) [23], chromium (Cr) [24] and copper (Cu) [25] have been used as dopants in many different studies. In our previous studies, photovoltaic properties of solar cell structures such as $\text{TiO}_2 / \text{Fe}: \text{ZnS}$ [26] $\text{TiO}_2 / \text{Cr}: \text{CdS}$ [24], $\text{Zn}_2\text{SnO}_4/\text{Mn}: \text{ZnS}$ [27] have been investigated and it has been reported that the doped devices have better solar cell performance than un-doped devices. Thus, it can be said that the doping plays a significant role to boost the efficiency of semiconductor-based solar cells.

It is possible to synthesize semiconductor thin films by applying many different techniques. In previous different studies [17, 28], Sb_2S_3 thin films have been synthesized by chemical bath deposition (CBD) method. One of the main reasons for using this technique is low cost. It was also emphasized that the desired Sb_2S_3 thin films were synthesized without the need for intensive laboratory conditions.

In this present study, Ni-doped Sb_2S_3 thin films with different Ni concentrations were synthesized on Zn_2SnO_4 coated with FTO conductive glasses by CBD method at room temperature using Ni as the dopant material. The concentration of Ni to be doped during the experiment was determined as 0.25%, 0.5%, 0.75%, and 1%. In the first stage of this study, incident photon to electron conversion efficiency (IPCE) and current density (J)- voltage (V) measurements were conducted to investigate the photovoltaic properties of $\text{Zn}_2\text{SnO}_4 / \text{Ni}$ -doped Sb_2S_3 thin films with different Ni concentrations for the first time. The main reason for performing IPCE and J-V measurements is to determine Ni-doped Sb_2S_3 thin film with optimum Ni concentration which shows the best solar cell performance.

After determining the optimum Ni concentration, the structural, optical and elemental properties of Ni-doped Sb_2S_3 thin films with this concentration were investigated, respectively.

2. Experimental part

2.1 Synthesis of Zn_2SnO_4 nanoparticles

The method used for the synthesis of nanoparticles is the hydrothermal technique. 50 ml of zinc acetate dehydrate ($\text{Zn}(\text{CH}_3\text{COO})_2 \cdot 2\text{H}_2\text{O}$) aqueous solution and 50 ml of tin chloride pentahydrate ($\text{SnCl}_4 \cdot 5\text{H}_2\text{O}$) aqueous solution was stirred at room temperature. The stirring process was continued until to get a homogeneous mixture. Then, sodium hydroxide (NaOH) solution was dropped on the mixture. The obtained white slurry precipitation was transferred into 200 ml Teflon coated autoclave. The autoclave was kept at 180°C for 12 h in an oven. The product was filtered washed and dried in a hot air oven. Thus, the formation of Zn_2SnO_4 nanoparticles was obtained.

To be formed Zn_2SnO_4 coated on fluorine alloyed tin oxide (FTO, $13\Omega \cdot \text{sq}^{-2}$) conductive glasses The Zn_2SnO_4 paste was coated on the FTO substrates using the doctor blade method, then sintered at 450°C for 45 minutes.

2.2 Synthesis of $\text{Zn}_2\text{SnO}_4 / \text{Sb}_2\text{S}_3$ thin films

In a typical CBD method, 0.65g of antimony chloride (SbCl_3) was dissolved in 10 ml of acetone. 25 mL of 1 M aqueous solution of sodium thiosulfate ($\text{Na}_2\text{S}_2\text{O}_3 \cdot 5\text{H}_2\text{O}$) was added to a solution containing SbCl_3 . The total volume of the mixture was made 100 mL by adding an appropriate amount of de-ionized water. After obtaining a homogeneous mixture, Zn_2SnO_4 coated on FTO substrate was vertically left into Sb_2S_3 solution for the certain time. Afterward, the substrate was removed from the chemical bath, washed well with de-ionized water and dried in air. The glass substrate was annealed at 350°C for 1 h under N_2 .

2.3 Synthesis of $\text{Zn}_2\text{SnO}_4 / \text{Ni}$ -doped Sb_2S_3 thin films with different Ni concentrations

For preparing $\text{Zn}_2\text{SnO}_4 / \text{Ni}$ -doped Sb_2S_3 thin films with different Ni concentrations, the different concentrations of nickel (II) nitrate hexahydrate ($\text{Ni}(\text{NO}_3)_2 \cdot 6\text{H}_2\text{O}$) were added 0.65g of SbCl_3 solution and then followed the same procedure mentioned above.

3. Characterizations

Incident photons to current efficiency (IPCE) and current density (J)- voltage (V) measurements were performed by using PCE-S20 with a monochromatic light source consisting of a 150-W Xe lamp and a monochromator. Structural properties of the thin film were characterized by x-ray diffraction on a Rigaku X-ray diffractometer with Cu K_{α} ($\lambda = 154,059$ pm) radiation. Optical characterization was performed by ultraviolet-visible on a Perkin-Elmer Lambda 2. The elemental analysis was studied by energy dispersive x-ray measurement (JEOL JSM 5800).

4. Results and discussions

4.1 IPCE and J-V measurements for Zn_2SnO_4 /Ni-doped Sb_2S_3 thin films with different Ni concentrations

The optimum concentration of Ni content in Zn_2SnO_4 /Ni-doped Sb_2S_3 thin films with different Ni concentrations was determined using the in IPCE and J-V measurements, respectively. The recorded IPCE spectra for Zn_2SnO_4 / Sb_2S_3 and Zn_2SnO_4 /Ni-doped Sb_2S_3 with different Ni concentrations are shown in Fig. 1.

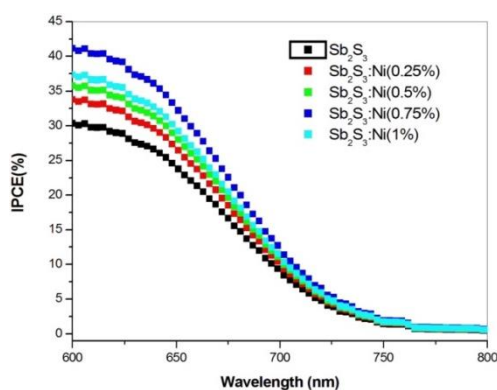


Fig. 1. The recorded IPCE spectra for Zn_2SnO_4 / Sb_2S_3 and Zn_2SnO_4 /Ni-doped Sb_2S_3 thin films with different Ni concentrations.

The obtained IPCE (%) values for Zn_2SnO_4 / Sb_2S_3 and Zn_2SnO_4 /Ni-doped Sb_2S_3 thin films with different Ni concentrations are given in Table 1.

Table 1. The obtained IPCE (%) values for thin films.

Thin films	The obtained IPCE (%) values at 600 nm
Sb_2S_3	30.40
Sb_2S_3 : Ni(0.25%)	33.84
Sb_2S_3 : Ni(0.5%)	35.59
Sb_2S_3 : Ni(0.75%)	41.00
Sb_2S_3 : Ni(1%)	37.16

It can be seen clearly, the efficiency of Zn_2SnO_4 / Sb_2S_3 thin film shows an enhancement when it is doped with Ni content. The optimum Ni concentration is 0.75% because the obtained maximum the IPCE (%) value efficiency is 41.00 % for Sb_2S_3 : Ni(0.75%) thin film. Consequently, it can be said that the Ni content plays an important role to boost the efficiency of Zn_2SnO_4 /Ni-doped Sb_2S_3 thin films with different Ni concentrations.

J-V measurements were applied to calculate power conversion efficiency values (η) of synthesized thin films. The power conversion efficiencies of the thin films were calculated using the recorded J-V curve.

Fig. 2 demonstrates the recorded J-V curves for $\text{Zn}_2\text{SnO}_4/\text{Sb}_2\text{S}_3$ and $\text{Zn}_2\text{SnO}_4/\text{Ni-doped Sb}_2\text{S}_3$ thin films with different Ni concentrations.

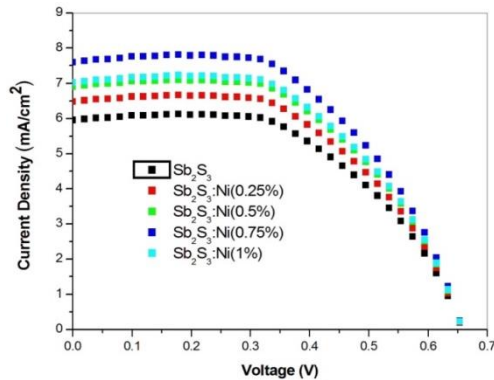


Fig. 2. The recorded J-V curves for $\text{Zn}_2\text{SnO}_4/\text{Sb}_2\text{S}_3$ and $\text{Zn}_2\text{SnO}_4/\text{Ni-doped Sb}_2\text{S}_3$ thin films with different Ni concentrations.

The obtained short-circuit current density (J_{SC}), open circuit voltage (V_{OC}) and $\eta\%$ values are given in Table 2.

Table 2. J_{SC} , V_{OC} and $\eta\%$ values $\text{Zn}_2\text{SnO}_4/\text{Sb}_2\text{S}_3$ and $\text{Zn}_2\text{SnO}_4/\text{Ni-doped Sb}_2\text{S}_3$ thin films with different Ni concentrations.

Thin films	J_{SC} (mA/cm ²)	V_{OC} (V)	$\eta\%$
Sb_2S_3	5.98	0.66	3.95
$\text{Sb}_2\text{S}_3:\text{Ni}(0.25\%)$	6.50	0.66	4.29
$\text{Sb}_2\text{S}_3:\text{Ni}(0.5\%)$	6.91	0.66	4.56
$\text{Sb}_2\text{S}_3:\text{Ni}(0.75\%)$	7.63	0.66	5.04
$\text{Sb}_2\text{S}_3:\text{Ni}(1\%)$	6.98	0.66	4.61

It should be noted that there is a significant improvement in the performance of the Sb_2S_3 thin film when it is doped with different concentrations of Ni.

As can be seen from Table 2, (1) the η (%) of $\text{Zn}_2\text{SnO}_4/\text{Ni-doped Sb}_2\text{S}_3$ thin films with different Ni concentrations is higher than $\text{Zn}_2\text{SnO}_4/\text{Sb}_2\text{S}_3$. The Ni dopant plays an effective role to enhance the performance of the $\text{Zn}_2\text{SnO}_4/\text{Sb}_2\text{S}_3$ -based solar cells. (2) The η (%) value of $\text{Sb}_2\text{S}_3:\text{Ni}(0.75\%)$ thin film has the highest value when the η (%) values of the four different Ni concentrations used are compared.

Thus, it was experimentally determined with the data obtained from the IPCE and J-V measurements that $\text{Sb}_2\text{S}_3:\text{Ni}(0.75\%)$ thin film has better efficiency than both the pure Sb_2S_3 and other Ni concentrations used.

4.2 XRD patterns for $\text{Sb}_2\text{S}_3:\text{Ni}(0.75\%)$ thin film

Fig. 3 indicates XRD patterns of $\text{Sb}_2\text{S}_3:\text{Ni}(0.75\%)$ thin film. The recorded all diffraction patterns for $\text{Sb}_2\text{S}_3:\text{Ni}(0.75\%)$ thin film can be identified as those of orthorhombic, Sb_2S_3 . The diffraction patterns are located at $2\theta^\circ = 15.48, 17.27, 21.95, 24.64, 28.06, 29.14,$

$32.01, 35.06, 36.68, 39.01, 39.91,$ and 42.60 and associate with (020), (120), (220), (130), (230), (211), (221), (301), (231), (430), (141), and (421) planes, respectively, of the orthorhombic Sb_2S_3 . Any XRD patterns related to Ni compounds or oxides are not observed. The average size of

the Sb_2S_3 : Ni(0.75%) thin film, estimated from the full width at half height of diffraction peaks using the Debye-Scherrer formula, is 51.18 nm.

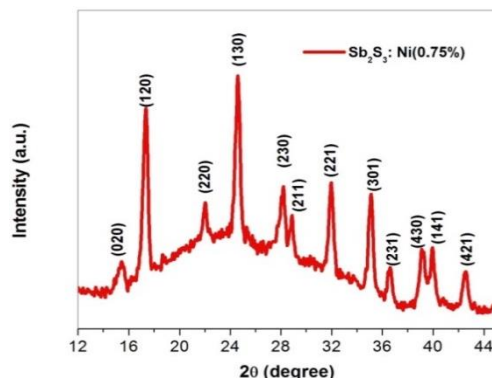


Fig. 3. The recorded XRD patterns of Sb_2S_3 : Ni(0.75%) thin film.

4.3 Determination energy band gap value for Sb_2S_3 : Ni(0.75%) thin film

UV-Vis spectroscopy was used to study the band structure of Sb_2S_3 : Ni(0.75%) thin film. Equation (1), called as Tauc's relation, was used to determine energy band gap value of Sb_2S_3 : Ni(0.75%) thin film.

$$\alpha h\nu = C(h\nu - E_g)^n \quad (1)$$

Where α is the absorption coefficient, $n=1/2$ or 2 for direct or indirect allowed transition, respectively, C is the characteristic parameter for respective transitions, $h\nu$ is photon energy and E_g is energy band gap.

The recorded optical absorption spectrum and $(\alpha h\nu)^2$ versus $h\nu$ curve for Sb_2S_3 : Ni(0.75%) thin film was demonstrated in Fig. 4(a-b).

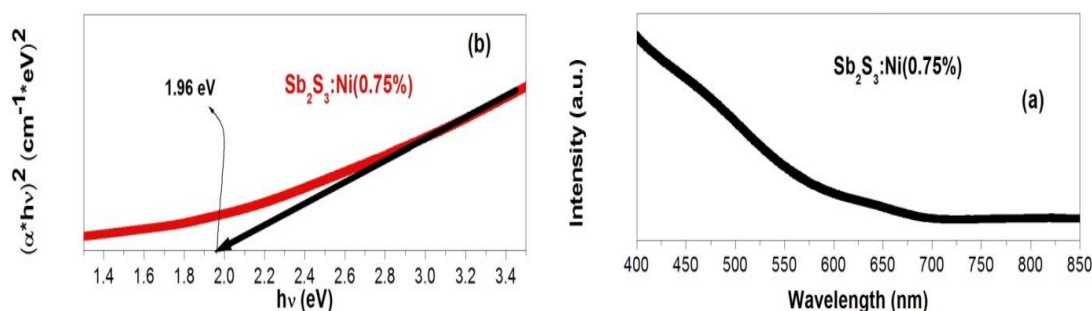


Fig. 4. (a) The recorded optical absorption spectrum and (b) $(\alpha h\nu)^2$ versus $h\nu$ curve for Sb_2S_3 : Ni(0.75%) thin film.

It was determined that the band gap value for Sb_2S_3 : Ni(0.75%) thin film is 1.96 eV whereas the band gap value for un-doped Sb_2S_3 thin film is 1.89 eV (is not shown). The obtained the band gap values for thin films show that the absorption wavelength (~ 642.48 nm) of Sb_2S_3 : Ni(0.75%) thin film is shifting to the shorter wavelength compared to pure Sb_2S_3 (~ 656.08 nm). The increase in energy band gap value of Sb_2S_3 : Ni(0.75%) thin film in the presence of Ni additive material, may be owing to structural modification. Furthermore, it can be said that the replacement of Ni ion in the Sb_2S_3 lattice is a reason for an increase in energy band gap value of Sb_2S_3 thin film. As a result, this situation could lead to being formed some additional energy levels in Sb_2S_3 energy band gap.

4.4 Determination of real % of nickel in Sb₂S₃: Ni(0.75%) thin film

The energy dispersive x-ray (EDX) spectrum was used to confirm the elemental compositions of Sb₂S₃: Ni(0.75%) thin film. The elemental percentages for thin film obtained from EDX patterns are 62.17 for Sb, 37.26 for S and 0.57 for Ni. Thus, this result can be an indication that the Ni additive material is successfully incorporated into Sb₂S₃.

5. Conclusions

We reported that Ni-doped Sb₂S₃ thin films with different Ni concentrations are synthesized on Zn₂SnO₄ coated with FTO conductive glasses by CBD method at room temperature. The concentration of Ni to be doped during the experiment was determined as 0.25%, 0.5%, 0.75%, and 1%. In the present study, IPCE and J-V measurements were conducted to investigate the photovoltaic properties of Zn₂SnO₄/Ni-doped Sb₂S₃ thin films with different Ni concentrations for the first time. The main reason for performing IPCE and J-V measurements is to determine Ni-doped Sb₂S₃ thin film with optimum Ni concentration which shows the best solar cell performance. It was observed that Sb₂S₃: Ni(0.75%) thin film has better efficiency ($\eta\%$ =5.04) than other Ni concentration.

Acknowledgments

This study supported by the Scientific and Technological Research Council of Turkey. (TUBITAK) (Project number: 117F193)

References

- [1] P. Kumar, L. Morawska, C. Martani, G. Biskos, M. Neophytou, S. D. Sabatino, M. Bell, L. Norford, R. Britter, *Environment International* **75**, 199 (2017).
- [2] A. Voinov, T. Filatova, *Frontiers of Earth Science* **8**, 3 (2014).
- [3] P. Zhang, W. Wang, Y. Yang, Y. Yao, L. Sun, *Angewandte Chemie* **126**, 14023 (2014).
- [4] S. E. Hosseini, M. A. Whaid, M. M. Jamil, A. A. M. Azli, M. F. Misbah, *International Journal of Energy Research* **39**, 1597 (2015).
- [5] M. J. Biermann, S. Jin, *Energy Environmental Science* **2**, 1050 (2009).
- [6] S. O. Stranks, H. J. Snaith, *Nature Nanotechnology* **10**, 391 (2015).
- [7] B. Maennig, J. Drechsel, D. Gebeyehu, P. Simon, F. Kozlowski, A. Werner, F. Li, S. Grundmann, S. Sonntag, M. Koch, K. Leo, M. Pfeiffer, H. Hoppe, D. Meissner, N. S. Sariciftci, I. Riedel, V. Dyakonov, J. Parisi, *Applied Physics A* **79**, 1 (2004).
- [8] X. Wang, L. Zhi, K. Muller, *Nano Letters* **8**, 323 (2008).
- [9] M. Yamaguchi, T. Takamoto, K. Araki, *Solar Energy Materials and Solar Cells* **90**, 3068 (2006).
- [10] S. H. Im, C. R. Lee, J. W. Lee, S. W. Park, N. G. Park, *Nanoscale* **3**, 4088 (2011).
- [11] M. Edoff, *Ambio* **41**, 112 (2012).
- [12] L. Yu, R. S. Kokenyesi, D. A. Keszler, A. Zunger, *Advanced Energy Materials* **3**, 43 (2012).
- [13] S. G. Deshmukh, S. J. Patel, K. K. Patel, A. K. Panchol, V. Kheraj, *Journal of Electronic Materials* **46**, 5582 (2017).
- [14] R. Parize, T. Cossuet, O. C. Pluchery, H. Roussel, E. Appert, V. Consonni, *Materials and Design*, **221**, 1 (2017).
- [15] P. A. Chate, S. D. Lakde, *International Journal of Thin Films Science and Technology* **4**, 237 (2015).
- [16] A. Arato, E. Cardenas, S. Shaji, J. J. O'Brien, J. Liu, G. A. Castillo, T. K. D. Ray, B. Krishnan, *Sb₂S₃:C/CdS p-n junction by laser irradiation* **517**, 2493 (2008).
- [17] M. T. S. Nair, Y. Pena, J. Campos, V. M. Garcia, P. K. Nair, *Journal of the Electrochemical*

- Society **145**, 2113 (1998).
- [18] S. M. Sze, *Physics of semiconductor devices*. Wiley, New York 1981.
- [19] S. Das, R. Aluguri, S. Manna, R. Singha, A. Dhar, L. Pavesi, S. K. Ray, *Nano Research Letters* **7**, 143 (2012).
- [20] N. Susha, R. J. Mathew, S. S. Nair, *Journal of Material Science* **51**, 10526 (2016).
- [21] M. S. A. Wahab, A. Jilani, I. S. Vahia, A. A. A. Ghmadi, *Superlattices and Microstructures* **94**, 108 (2016).
- [22] W. A. A. Syed, N. Rafiq, W. H. Shah, S. Shah, N. Ali, *Chalcogenide Letters* **14**, 259 (2017).
- [23] A. Javed, Q. U. Ain, M. Bashir, *Journal of Alloys and Compounds* **759**, 14 (2018).
- [24] S. Horoz, O. Sahin, *Journal of Materials Science: Materials in Electronics* **28**, 17784 (2017).
- [25] D. E. O. Ramos, L. A. Gonzales, R. R. Bon, *Materials Letters* **124**, 267 (2014).
- [26] S. Horoz, O. Sahin, *Journal of Materials Science: Materials in Electronics* **28**, 9559 (2017).
- [27] S. Horoz, Q. Dai, S. Maloney, B. Yakami, J. Pikal, X. Zhang, J. Wang, W. Wang, J. Tang, *Physical Review Applied* **3**, 014011 (2015).
- [28] Y. Itzhaik, O. Niitsoo, M. Page, G. Hodes, *The Journal of Physical Chemistry C* **113**, 4254 (2009).